Numerical computations for the Schramm-Loewner Evolution

Tom Kennedy
Department of Mathematics
University of Arizona
Tucson, AZ 85721
email: tgk@math.arizona.edu

June 25, 2018

Abstract

We review two numerical methods related to the Schramm-Loewner evolution (SLE). The first simulates SLE itself. More generally, it finds the curve in the half-plane that results from the Loewner equation for a given driving function. The second method can be thought of as the inverse problem. Given a simple curve in the half-plane it computes the driving function in the Loewner equation. This algorithm can be used to test if a given random family of curves in the half-plane is SLE by computing the driving process for the curves and testing if it is Brownian motion. More generally, this algorithm can be used to compute the driving process for random curves that may not be SLE. Most of the material presented here has appeared before. Our goal is to give a pedagogic review, illustrate some of the practical issues that arise in these computations and discuss some open problems.

1 Introduction

This review is about two types of numerical calculations related to the Schramm-Loewner evolution (SLE). The first is to simulate SLE itself. More generally, one can consider simulating the random curves you obtain in the plane when a random process is used for the driving function in the Loewner equation. The second type of simulation is to take a family of random curves in the plane and compute the random driving process that generates them through the Loewner equation. This is related to SLE since one can test if a given family of random curves is SLE by testing if the random driving process is Brownian motion. More generally, it is of interest to study the random driving process for random curves that may not be SLE. This review is meant to be pedagogic. Most of this material has appeared elsewhere. Our goal is to provide the reader with a "how-to" guide that will enable him or her to do state of the art simulations related to SLE.

In the next section we give a heuristic and somewhat atypical introduction to SLE that does not involve the Loewner equation. This is followed in section 3 with a quick review of the Loewner equation and the usual definition of SLE. The "discretization" of SLE that is used in section 2 and discussed in detail in section 3 was studied extensively in [2] for a particular approximation of the driving function (vertical slits). Reviews of SLE from the mathematics point of view include [15, 23] and from the physics point of view include [3, 9, 11].

In section 4 we consider the numerical algorithm for finding a curve for a given driving function in the Loewner equation. Doing this with samples of Brownian motion for the driving function gives a simulation of SLE.

In section 5 we consider the numerical algorithm for finding the driving function for a given curve. One motivation for doing this is that it gives a way to test if a given model is SLE by testing if the driving process is Brownian motion. Several works have considered models for which the connection with SLE is not clear, including domain walls in spin glasses [1, 7] and turbulence [5, 6]. Another motivation is to study the driving process for massive scaling limits of off-critical models [4, 8, 18]

Both of the numerical algorithms we study are closely related to the zipper algorithm [14, 16]. This is an algorithm for numerically finding the conformal map of a given simply connected domain onto a standard domain such as the unit disc. Much of the work described in this review grew out of conversations with Don Marshall and Stephen Rohde.

2 An introduction to SLE

In this section we will give a heuristic introduction to SLE. The standard definition of SLE uses the Loewner equation from complex analysis. We will give a different definition of the process that does not use the Loewner equation. This view of SLE is well known, but is not typically discussed in reviews of SLE. The approach to SLE that we present is closely related to the numerical algorithms we will discuss. In the next section we will see how this approach is related to the usual definition using the Loewner equation.

Let \mathbb{H} denote the upper half of the complex plane,

$$\mathbb{H} = \{z : Im(z) > 0\} \tag{1}$$

Fix an angle $\theta \in (0, \pi/2]$ and a length $\rho > 0$. Let $f_+(z)$ be the conformal map which takes \mathbb{H} onto $\mathbb{H} \setminus \{re^{i\theta} : 0 < r \le \rho\}$, the upper half plane minus the line segment from 0 to $\rho e^{i\theta}$. This map is not unique. We make the choice unique by requiring

$$f_{+}(\infty) = \infty$$

$$f'_{+}(\infty) = 1$$

$$f_{+}(0) = \rho e^{i\theta}$$
(2)

The first two conditions mean that the Laurent series of f_+ about ∞ is of the form

$$f_{+}(z) = z + c_0 + \frac{c_1}{z} + \frac{c_2}{z^2} + \cdots$$

(For the reader familiar with the Loewner equation, we note that this is not the "hydrodynamic" normalization which would require that $c_0 = 0$ in the Laurent expansion instead of the third condition in (2).) The map f_+ is illustrated by the upper left picture in figure 1. The grid shown is the image under the conformal map of the uniform rectangular grid in the upper half plane. Let $f_-(z)$ be the analogous conformal map for the segment from 0 to $\rho e^{i(\pi-\theta)}$. (So the range of f_- is the reflection of the range of f_+ about the vertical axis.)

Consider composing two of these maps, e.g., $f_+ \circ f_-$. The effect of the second map in the composition will be to push the line segment created by the first map into the upper half plane and bend it somewhat. Because we have required that these maps send 0 to the tip of the line segment, the lower endpoint of the image of the first slit under the second map will be the tip of the second slit. In other words the image of \mathbb{H} under the composition will be \mathbb{H} with a curve removed. The map $f_+ \circ f_-$ is illustrated by the picture in the upper right of figure 1.

We can compose multiple copies of f_- and f_+ and the resulting conformal map will send the half plane onto the half plane minus a curve. We choose the maps randomly. Let X_n be a sequence of independent, identically distributed random variables with $X_n = \pm 1$ with probability 1/2. For positive integers n consider the conformal map

$$F_n = f_{X_1} \circ f_{X_2} \circ f_{X_3} \circ \dots \circ f_{X_n} \tag{3}$$

(There is a slight abuse of notation here: $f_{\pm 1}$ means f_{\pm} .) The picture in the lower left of figure 1 illustrates an example of F_5 , and the picture in the lower right an example of F_{10} .

The conformal map F_n will map \mathbb{H} onto $\mathbb{H} \setminus \hat{\gamma}_n$ where $\hat{\gamma}_n$ is a curve in the upper half plane starting at 0. Because of the order of the $X_i's$ in (3), the curve $\hat{\gamma}_{n+1}$ will be an extension of the curve $\hat{\gamma}_n$. So we can let $n \to \infty$ to get an infinite curve $\hat{\gamma}$. The SLE curve is then obtained by taking the scaling limit $\rho \to 0$. The angle α is related to the usual parameter κ for SLE. Using results that will appear latter, one can show that the relation is

$$\kappa = \frac{4(2\alpha - 1)^2}{\alpha(1 - \alpha)}$$

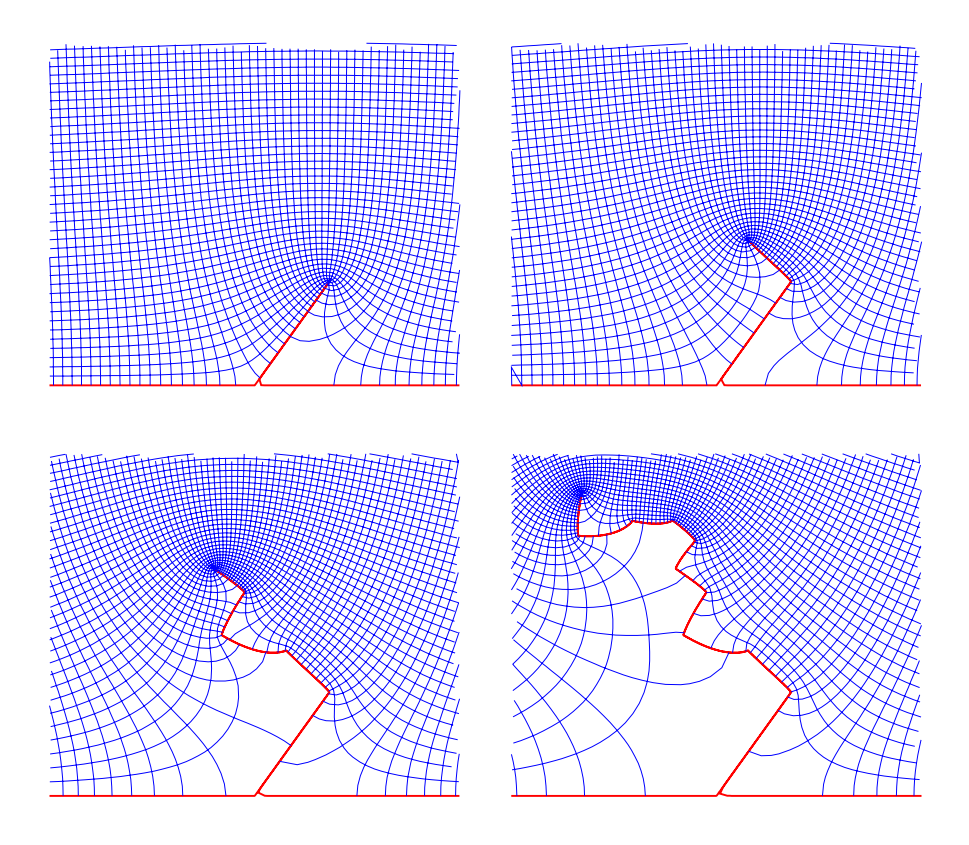


Figure 1: The figures illustrate the random composition of a sequence from the maps f_{-} and f_{+} . The numbers of maps in the compositions are 1, 2, 5 and 10.

When we use a piecewise smooth approximation to the driving function in the Loewner equation, the curve $\hat{\gamma}$ will be simple (non-intersecting). It is a subtle question whether the curves one obtains in the limit $\rho \to 0$ are simple. For $\kappa \le 4$, SLE produces a simple curve [20], and it is natural to conjecture that $\hat{\gamma}$ converges to this SLE curve. We do not prove this, and we are not aware of any proof in the literature. For $\kappa > 4$ the random set produced by SLE is not even a curve [20]. It is generated by a non-simple curve, called the SLE trace, in the sense that the SLE set at time t is the complement of the unbounded connected component of the half plane minus the curve up to time t. It is natural to conjecture that $\hat{\gamma}$ converges in distribution to the SLE trace, but again we do not prove this and are not aware of any proof in the literature. Closely related questions are considered in [2].

3 The Loewner equation

We will now quickly review the Loewner equation from complex analysis and see how it is related to the definition of SLE that we gave in the previous section. The Loewner equation provides a means for encoding curves in the upper half plane that do not intersect themselves by a real-valued function. In fact, it applies to more general growth processes in the half plane, but for the moment we restrict our attention to curves. Let $\gamma(t)$ be a simple curve which lies in \mathbb{H} for $0 < t < \infty$ and starts at the origin, i.e., $\gamma(0) = 0$. Let $\gamma[0, t]$ denote the image of γ up to time t. Then $\mathbb{H} \setminus \gamma[0, t]$ is a simply connected domain. So there is a conformal map g_t from this domain to \mathbb{H} . This map is not unique. We choose the map that satisfies

$$g_t(z) = z + \frac{C(t)}{z} + O(\frac{1}{|z|^2}), \qquad z \to \infty$$
(4)

The coefficient C(t) is called the half-plane capacity of $\gamma[0,t]$. It is known to be increasing in t, so we can parametrize the curve so that C(t) = 2t. Then g_t satisfies Loewner's differential equation

$$\frac{\partial g_t(z)}{\partial t} = \frac{2}{g_t(z) - U_t}, \qquad g_0(z) = z \tag{5}$$

for some real valued function U_t on $[0, \infty)$. This statement is not obvious, and we refer the reader to [15] for a proof. The function U_t is often called the driving function. We emphasize that while $g_t(z)$ is complex valued, the driving function U_t is real-valued.

Note that g_t goes in the opposite direction of the maps in the previous section, i.e., it sends the half plane with a curve deleted onto the half plane while the previous maps sent the half plane onto the half plane minus a curve. We should also note that g_t is normalized differently since the constant term in (4) vanishes. So $g_t(\gamma(t))$ is not the origin. In fact it is U_t . (To be precise, $g_t(\gamma(t))$ is not defined since $\gamma(t)$ is on the boundary of the domain of g_t . Its image under g_t must be defined by a limiting process.)

If our simple curve in the half plane is random, then the driving function U_t is a stochastic process. Schramm's wonderful discovery was that if the scaling limit of a two-dimensional model is conformally invariant and satisfies a property usually called the domain Markov property, then this stochastic driving process must be a Brownian motion with mean zero [21]. The only thing that is not determined is the variance. Schramm named this process stochastic Loewner evolution or SLE; it is now often referred to as Schramm-Loewner evolution.

The solution to (5) need not exist for all times t since the denominator can go to zero. We let K_t be the set of points z in \mathbb{H} for which the solution to this equation no longer exists at time t. If we start with a simple curve and define g_t as we did above, then K_t will be $\gamma[0,t]$. But if we start with a continuous driving function U_t and solve the Loewner equation, K_t will only be a curve for sufficiently nice U_t . (Just what sufficiently nice means is a subtle question [17].) For other U_t , K_t can be a more complicated growing set. In particular, when U_t is a Brownian motion, K_t may not be a curve. In our simulations, even in the cases where U_t is not sufficiently nice, our approximation to U_t will be nice enough that it produces a curve. So in

the following we will always take K_t to be a curve, but the reader should keep in mind that in some cases this curve is approximating a more complicated set.

Let t, s > 0. The map g_{t+s} maps $\mathbb{H} \setminus \gamma[0, t+s]$ onto \mathbb{H} . We can do this in two steps. We first apply the map g_s . This maps $\mathbb{H} \setminus \gamma[0, s]$ onto \mathbb{H} , and it maps $\mathbb{H} \setminus \gamma[0, t+s]$ onto $\mathbb{H} \setminus g_s(\gamma[s, t+s])$. Let \bar{g}_t be the conformal map that maps $\mathbb{H} \setminus g_s(\gamma[s, t+s])$ onto \mathbb{H} with the usual hydrodynamic normalization. Then $\bar{g}_t \circ g_s$ will map $\mathbb{H} \setminus \gamma[0, t+s]$ onto \mathbb{H} and satisfy (4). There is only one such conformal map, so

$$g_{s+t} = \bar{g}_t \circ g_s, \quad i.e., \quad \bar{g}_t = g_{s+t} \circ g_s^{-1} \tag{6}$$

It we think of s as being fixed and t as the time variable, then the function \bar{g}_t is also a solution of the Loewner equation

$$\frac{d}{dt}\bar{g}_t(z) = \frac{d}{dt}g_{s+t} \circ g_s^{-1}(z) = \frac{2}{g_{s+t} \circ g_s^{-1}(z) - U_{s+t}} = \frac{2}{\bar{g}_t(z) - U_{s+t}}$$
(7)

and satisfies $\bar{g}_0(z) = z$. Thus $\bar{g}_t(z)$ is obtained by solving the Loewner equation with driving function $\bar{U}_t = U_{s+t}$. This driving function starts at U_s , and so the curve associated with \bar{g}_t starts at U_s .

We now introduce a partition of the time interval $[0, \infty)$: $0 = t_0 < t_1 < t_2 < \cdots t_n < \cdots$, and define

$$\bar{g}_k = g_{t_k} \circ g_{t_{k-1}}^{-1} \tag{8}$$

So

$$g_{t_k} = \bar{g}_k \circ \bar{g}_{k-1} \circ \bar{g}_{k-2} \circ \dots \circ \bar{g}_2 \circ \bar{g}_1 \tag{9}$$

By the remarks above, \bar{g}_k is obtained by solving the Loewner equation with driving function $U_{t_{k-1}+t}$ for t=0 to $t=\Delta_k$, where $\Delta_k=t_k-t_{k-1}$. The image of \mathbb{H} under \bar{g}_k is \mathbb{H} minus a "cut" starting at $U_{t_{k-1}}$. So if we shift it by defining

$$g_k(z) = \bar{g}_k(z + U_{t_{k-1}}) - U_{t_{k-1}}, \tag{10}$$

then g_k is obtained by solving the Loewner equation with driving function $U_{t_{k-1}+t} - U_{t_{k-1}}$ for t = 0 to $t = \Delta_k$. This driving function starts at 0 and ends at δ_k where $\delta_k = U_{t_k} - U_{t_{k-1}}$. So this conformal map takes \mathbb{H} minus a cut starting at the origin onto \mathbb{H} . The inverse of this map,

$$g_k^{-1}(z) = \bar{g}_k^{-1}(z + U_{t_{k-1}}) - U_{t_{k-1}}, \tag{11}$$

takes H and introduces a cut which begins at the origin.

There are two general types of simulations we would like to do. Given a driving function we want to find the curve it generates. And given a curve we want to find the corresponding driving function. For both problems the key idea is the same. We approximate the driving function on the interval $[t_{k-1}, t_k]$ by a function for which the Loewner equation may be explicitly solved. So the maps \bar{g}_k and g_k can be found explicitly. Eq. (9) can then be used to approximate g_t . We will consider two explicit solutions of the Loewner equation which we will refer to as "tilted slits" and "vertical slits."

For tilted slits, let $x_l, x_r > 0$ and $0 < \alpha < 1$. Then define

$$f(z) = (z + x_l)^{1-\alpha} (z - x_r)^{\alpha},$$

Then f maps \mathbb{H} to $\mathbb{H} \setminus \Gamma$ where Γ is a line segment from 0 to a point $\rho e^{i\alpha\pi}$. The length ρ can be expressed in terms of x_l, x_r and α . This map sends $[-x_l, x_r]$ onto Γ . Unfortunately, its inverse cannot be explicitly computed. For the inverse to satisfy the normalization (4), we must have

$$(1 - \alpha)x_l = \alpha x_r \tag{12}$$

Straightforward calculation shows if we let

$$f_t(z) = \left(z + 2\sqrt{t}\sqrt{\frac{\alpha}{1-\alpha}}\right)^{1-\alpha} \left(z - 2\sqrt{t}\sqrt{\frac{1-\alpha}{\alpha}}\right)^{\alpha}$$

then it produces a slit with capacity 2t. We know that $g_t = f_t^{-1}$ must satisfy the Loewner equation (5) for some driving function U_t . More calculation shows that the driving function is

$$U_t = c_{\alpha} \sqrt{t}, \qquad c_{\alpha} = 2 \frac{1 - 2\alpha}{\sqrt{\alpha(1 - \alpha)}}$$
 (13)

The change in the driving function over the time interval $[0, \Delta]$ is

$$\delta = c_{\alpha} \sqrt{\Delta} \tag{14}$$

The original map ϕ had three real degrees of freedom, α, x_l, x_r . The condition (12) reduces this to two real degrees of freedom, α and t. So if we are given δ and Δ or given ρ and α , then the map is completely determined.

Vertical slits correspond to an even simpler solution of the Loewner equation. Let

$$g_t(z) = \sqrt{(z-\delta)^2 + 4t} + \delta$$

Then it is easy to check that g_t satisfies Loewner's equation with a constant driving function, $U_t = \delta$. Since the driving function does not start at 0, the curve will not start at the origin. The curve is just a vertical slit from δ to $\delta + 2i\sqrt{t}$. Using vertical slits means that we approximate the driving function by a discontinuous piecewise constant function. This will produce a K_t which is not a curve.

Our numerical studies only use tilted slits and vertical slits for the explicit solutions for the Loewner equation. Another possibility is to use a linear driving function. If we let $h_t = g_t - U_t$, then the differential equation for h_t can be solved by separation of variables. The solution is not completely explicit - it must be expressed in terms of a function that is defined implicitly by a transcendental equation.

4 From the driving function to the curve

Our primary motivation is to simulate SLE, i.e., to compute the curve when the driving function is Brownian motion. But our discussion is more general, and the following algorithm can be used to calculate the curve corresponding to any driving function U_t .

There are a variety of conformal maps that occur in this paper, and we have denoted them by letters that indicate what they do. Maps denoted with g are solutions of the Loewner equation with a driving function that starts at 0. So they map the half plane minus a curve starting at the origin onto the half plane, sending the tip of the curve to the final value of the driving function. We use \bar{g} for solutions to the Loewner equation when the driving function does not start at 0. In this case the curve starts at the initial value of the driving function and the map still sends the tip to the final value of the driving function. If we follow a map g by a real translation that takes the final value of the driving function to 0, we get a map that takes the half plane minus a curve onto the half plane and sends the tip to the origin. We denote such maps by h. (Note that such maps do not satisfy the Loewner equation.) Finally, we use f to denote maps that are inverses of maps h. So they take the half plane onto the half plane minus a curve and sends the origin to the tip.

Let $0 = t_0 < t_1 < t_2 < \cdots < t_n$ be a partition of the time interval [0, t]. The SLE curve is given by $\gamma(t) = g_t^{-1}(U_t)$. Let $z_k = g_{t_k}^{-1}(U_{t_k})$. We will only consider the points z_k on this curve which correspond to times $t = t_k$. One could consider other points on the curve, but the distance between consecutive z_k is already of the order of the error in our approximation, so there is no reason to consider more points. By (9) the points z_k are given by

$$z_k = \bar{g}_1^{-1} \circ \bar{g}_2^{-1} \circ \dots \bar{g}_{k-1}^{-1} \circ \bar{g}_k^{-1}(U_{t_k})$$
(15)

Recall that if we solve the Loewner equation with driving function $U_{t_{k-1}+t} - U_{t_{k-1}}$ for t = 0 to $t = \Delta_k$, the result is $g_k(z)$ where

$$g_k(z) = \bar{g}_k(z + U_{t_{k-1}}) - U_{t_{k-1}}$$
(16)

Define

$$h_k(z) = g_k(z) - \delta_k = \bar{g}(z + U_{t_{k-1}}) - U_{t_k}$$
(17)

where $\delta_k = U_{t_k} - U_{t_{k-1}}$. Then

$$h_k \circ h_{k-1} \circ \cdots \circ h_1(z_k) = \bar{g}_k \circ \bar{g}_{k-1} \circ \cdots \circ \bar{g}_1(z_k) - U_{t_k} = 0.$$
 (18)

Let

$$f_k = h_k^{-1} \tag{19}$$

So

$$z_k = f_1 \circ f_2 \circ \dots \circ f_k(0) \tag{20}$$

As noted before, g_k maps \mathbb{H} minus a small curve onto \mathbb{H} . The driving function ends at δ_k , so g_k sends the tip of the curve to δ_k . It follows that $h_k(z) = g_k(z) - \delta_k$ maps \mathbb{H} minus the

small curve onto \mathbb{H} and sends the tip to the origin. So $f_k = h_k^{-1}$ maps \mathbb{H} onto \mathbb{H} minus the small curve and sends the origin to the tip of the curve. Thus the functions f_k are analogous to the functions f_{\pm} from section 2 in that they all introduce a small cut into the upper plane and send the origin to the tip of the cut. Note the similarity of (20) to (3).

As discussed before, we define U_t on each time interval $t_{k-1} \leq t \leq t_k$ so that $g_k(z)$ may be explicitly computed. There are two constraints on g_k . The curve must have capacity $2\Delta_k$ and g_k must map the tip of the curve to δ_k . Any simple curve satisfying these two constraints and starting at the origin will correspond to a solution of the Loewner equation for some driving function which goes from 0 to δ_k over the time interval $[0, \Delta_k]$. So our approximation can be thought of as replacing the driving function by a new driving function that agrees with the original one at the times t_k but differs in between those times.

Different choices of how we define U_t on each time interval give us different discretizations. As we will see, this choice will not have a significant effect. Of much greater importance is how we choose the Δ_k and δ_k .

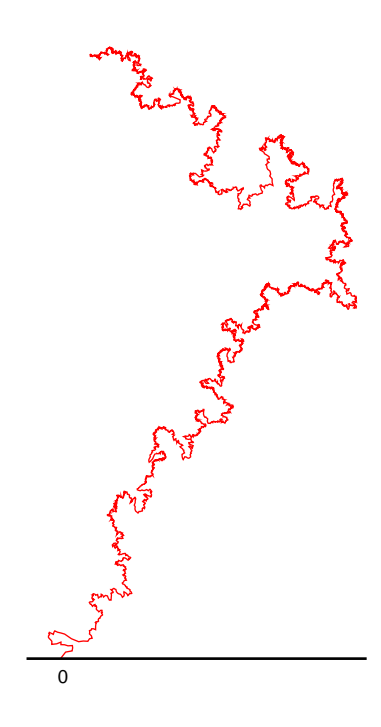


Figure 2: SLE with $\kappa = 8/3$ with fixed Δt . There are 10,000 points.

If we want to simulate SLE, the δ_k should be chosen so that the stochastic process U_t will converge to $\sqrt{\kappa}$ times Brownian motion as $N \to \infty$. One choice is take the δ_k to be independent normal random variables with mean zero and variance $\kappa \Delta_k$. If we do this, then U_t and $\sqrt{\kappa}B_t$ will have the same distributions if we only consider the times t_k . Another possibility is to approximate the Brownian motion by a simple random walk. This is done by using a uniform partition of the time interval and taking the δ_k to be independent random variables

with $\delta_k = \pm \sqrt{\kappa \Delta_k}$ where the choices of + and - both have probability 1/2. This is what we were doing in section 2.

The simplest choice for Δ_k is to use a uniform partition of the time interval. For values of κ which are not too large this works reasonably well. Figure 2 shows a simulation using $\kappa = 8/3$ with 10,000 equally spaced time intervals. However, for larger values of κ , uniform Δ_k are a disaster. Figure 3 shows a simulation with $\kappa = 6$ and 10,000 equally spaced time intervals. Clearly something has gone wrong. To see just how badly wrong things have gone the reader should compare this figure with figure 4 which uses the same sample of Brownian motion.

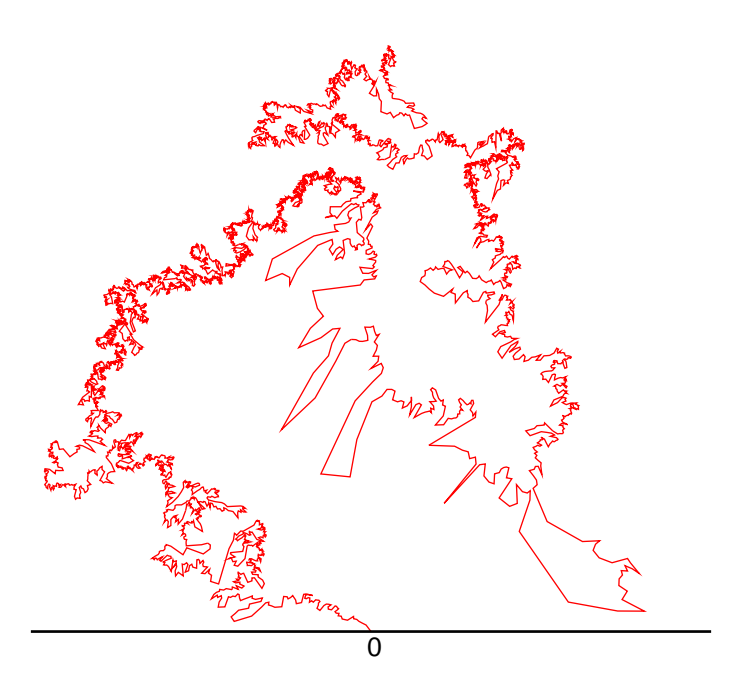


Figure 3: SLE with $\kappa = 6$ with fixed Δt . There are 10,000 points.

To understand the effect seen in figure 3 we give an equivalent definition of the half plane capacity C of a set A. We originally defined it by

$$g(z) = z + \frac{C}{z} + O(\frac{1}{z^2})$$

where g maps $\mathbb{H} \setminus A$ onto \mathbb{H} . A more intuitive definition is

$$C = \lim_{y \to \infty} y \, E^{iy} [Im(B_\tau)]$$

where B_t is two-dimensional Brownian motion started at iy. The stopping time τ is the first time the Brownian motion hits A or \mathbb{R} . From the point of view of this two-dimensional Brownian motion, parts of the curve can be well hidden by earlier parts of the curve and so have very

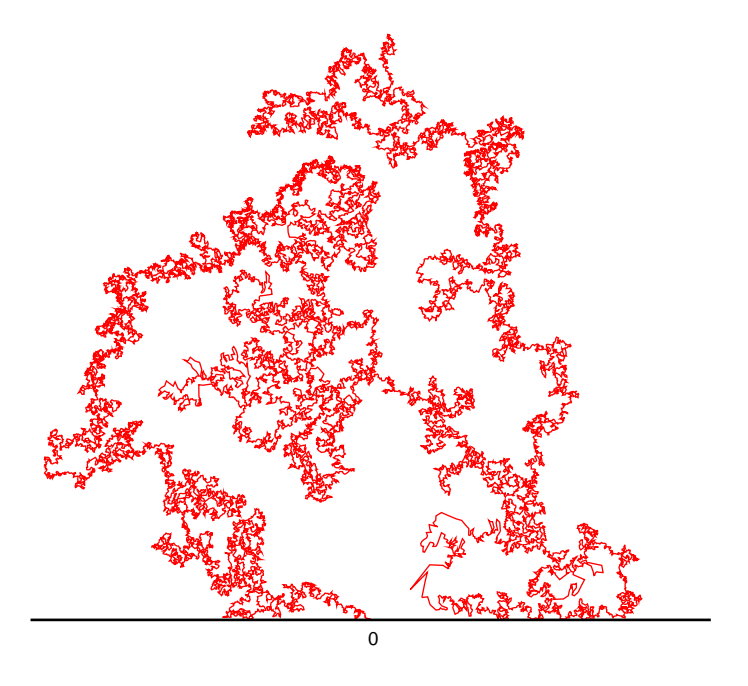


Figure 4: SLE with $\kappa = 6$ with adaptive Δt . There are 35,000 points.

little capacity. So what looks like a "long" section of the curve has very little capacity and so gets very few points approximating it.

To do better we will use non-uniform Δ_k . In fact they will depend on the sample of the Brownian motion and so we refer to this method as "adaptive Δ_k ." (I learned this idea from Stephen Rohde [19].) Fix a spatial scale $\epsilon > 0$. We start with a uniform partition of the time and compute the points z_k along the curve. Then we look for points z_k such that $|z_k - z_{k-1}| \ge \epsilon$. For these time intervals $[t_{k-1}, t_k]$, divide the interval into two equal intervals. We then sample the Brownian motion at the midpoint of $[t_{k-1}, t_k]$ using a Brownian bridge. (This just means that to choose the value of the driving function at the midpoint of $[t_{k-1}, t_k]$ we use a Brownian motion conditioned on the values we already have for it at t_{k-1} and t_k .) Then we recompute all the z_k . (There will of course be more of them than before.) Note that we must recompute all the points since even at times which appeared in the time partition before, the corresponding point on the curve will change. We repeat this until we have $|z_k - z_{k-1}| \le \epsilon$ for all k.

Our approximation can be thought of as approximating the driving function by a concatenation of driving functions on short time intervals for which the Loewner equation is exactly solvable. It is important to consider the effect of the choice of which exactly solvable driving functions we use. To do this we compare the curves we get using tilted slits for the elementary maps with the curves we get using vertical slits. We carry out the adaptive simulation just described using tilted slits. We then use the same Δ_k and δ_k , i.e., the same partition of the time interval and the same sample of Brownian motion, but with vertical slits. For $\kappa = 8/3$, figure 5 shows the tilted slits curve vs. the vertical slits curve. The vertical slits do not produce a curve. What we have plotted is the following. We compute the points z_k and then just connect them with a straight line. In figure 5 it is almost impossible to distinguish the two curves. An enlargement of part of the curves is shown in the inset. Even in the enlargement the difference is quite small. The curves have a relatively small number of points (about 6,000), and in the enlargement we have plotted the points for the tilted slit curve. The difference between the two curves is on the order of the distance between these points.

Figure 6 shows the same thing with $\kappa = 6$. In the enlargement one can see deviations between the two curves, but the size of the deviations is again on the same scale as the distance between adjacent points on the curve.

It is interesting to note that there is what one might call a stability to the approximation we are using. The difference between the two curves in figures 5 and 6 fluctuates with time, but it does not grow with time. In other words, the errors from approximating the true driving function over the short time intervals do not appear to accumulate.

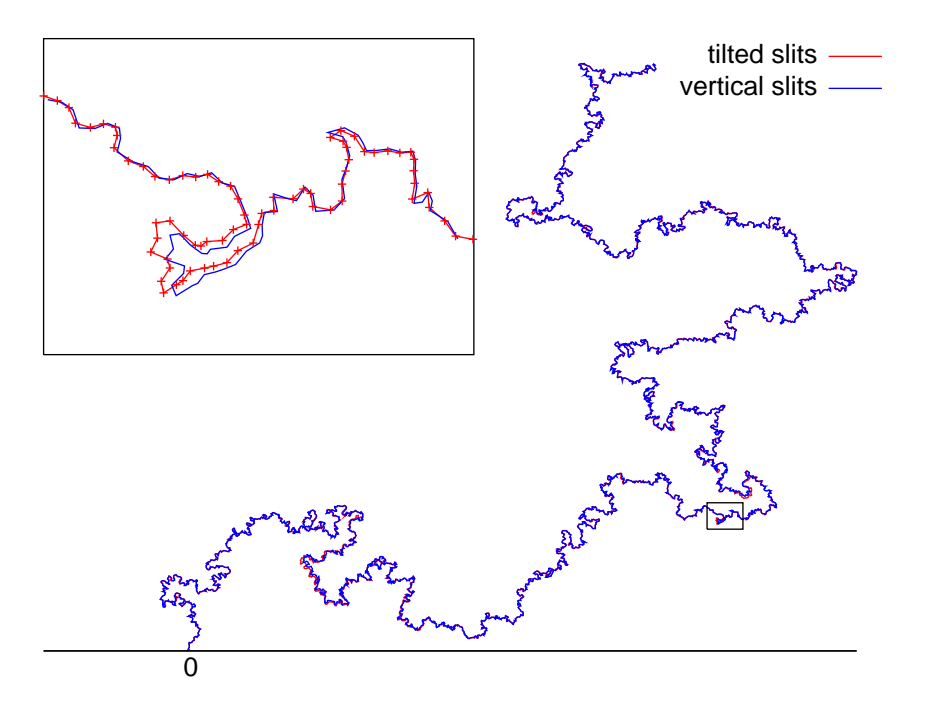


Figure 5: A comparison of the curves obtained using tilted slit maps and vertical slit maps with $\kappa = 8/3$.

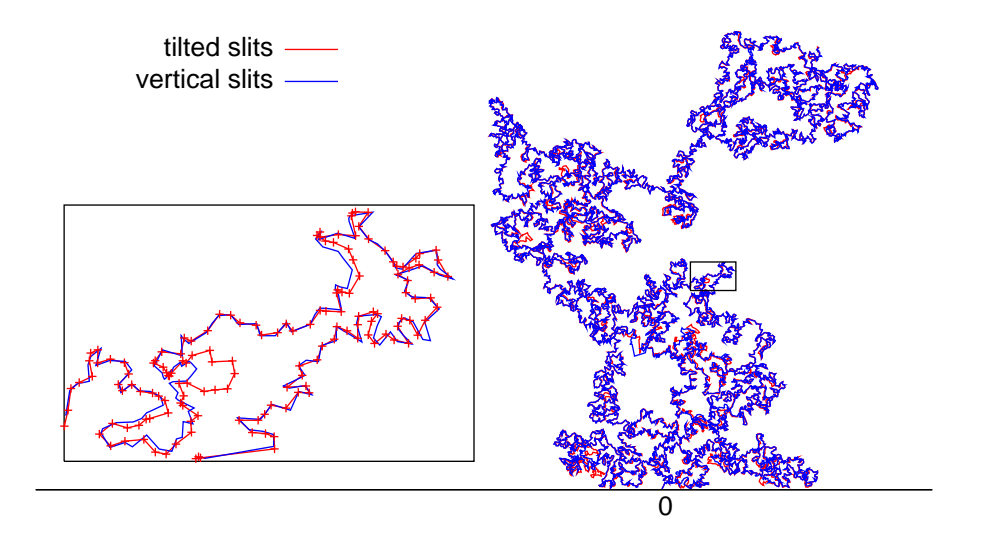


Figure 6: A comparison of the curves obtained using tilted slit maps and vertical slit maps with $\kappa=6$.

5 From the curve to the driving function

We now consider what one might call the inverse problem. Given a simple curve γ , we want to compute the corresponding driving function.

Let $\gamma(s)$ be a parametrized simple curve in \mathbb{H} . In almost all applications, the parametrization of the curve is not the parametrization by capacity. Let g_s be the conformal map which takes $\mathbb{H} \setminus \gamma[0,s]$ onto \mathbb{H} , normalized so that for large z

$$g_s(z) = z + \frac{C(s)}{z} + O(\frac{1}{z^2}),$$
 (21)

The coefficient C(s) is the half-plane capacity of $\gamma[0, s]$. The value of the driving function at t = C(s)/2 is $U_t = g_s(\gamma(s))$. Thus computing the driving function essentially reduces to computing this uniformizing conformal map.

Let z_0, z_1, \dots, z_n be points along the curve γ with $z_0 = 0$. In many applications these are lattice sites. We will find a sequence of conformal maps h_i , $i = 1, 2, \dots, n$ such that $h_k \circ h_{k-1} \circ \cdots \circ h_1(z_k) = 0$. Then $h_k \circ h_{k-1} \circ \cdots \circ h_1$ sends $\mathbb{H} \setminus \hat{\gamma}$ to \mathbb{H} where $\hat{\gamma}$ is some curve that passes through z_0, z_1, \dots, z_k and so approximates γ . Suppose that the conformal maps h_1, h_2, \dots, h_k have been defined with these properties. Let

$$w_{k+1} = h_k \circ h_{k-1} \circ \dots \circ h_1(z_{k+1}) \tag{22}$$

Then w_{k+1} is close to the origin. We define h_{k+1} to be a conformal map that sends $\mathbb{H} \setminus \gamma_{k+1}$ to \mathbb{H} where γ_{k+1} is a short simple curve from 0 to w_{k+1} . We also require that h_{k+1} sends w_{k+1} to the origin. As before we choose the curve γ_{k+1} so that h_{k+1} is explicitly known; possible choices include "tilted slits" and "vertical slits." Note that for both of these maps there were two real degrees of freedom. They will be determined by the condition that $h_{k+1}(w_{k+1}) = 0$.

Let $2\Delta_i$ be the capacity of the map h_i , and δ_i the final value of the driving function for h_i . So

$$h_i(z) = z - \delta_i + \frac{2\Delta_i}{z} + O(\frac{1}{z^2})$$
(23)

Then

$$h_k \circ h_{k-1} \circ \dots \circ h_1(z) = z - U_t + \frac{2t}{z} + O(\frac{1}{z^2})$$
 (24)

where

$$t = \sum_{i=1}^{k} \Delta_i \tag{25}$$

$$U_t = \sum_{i=1}^k \delta_i \tag{26}$$

Thus the driving function of the curve is obtained by concatenating the driving functions of the elementary conformal maps h_i .

6 Faster algorithms

In this section we show how to speed up both the algorithm for computing the curve γ given the driving function U_t and the algorithm for computing the driving function U_t given a curve γ . We start with the first algorithm. One of the main motivations is a fast algorithm for simulating SLE, but our fast algorithm is applicable to other driving functions as well.

Recall that points on the approximation to the SLE trace or more generally the curve γ are given by eq. (20) which says

$$z_k = f_1 \circ f_2 \circ \dots \circ f_k(0) \tag{27}$$

The number of operations needed to compute a single z_k is proportional to k. So to compute all the points z_k with $k = 1, 2, \dots N$ requires a time $O(N^2)$. The computation of z_k does not depend on any of the other z_j . Depending on what we want to compute, we may only need to compute a subset of the points z_k . (For example, if we are only interested in $z_N = \gamma(t_N)$, the time required is O(N) not $O(N^2)$.) For a typical point z_k , the time to compute it is O(N) for the above algorithm. Our goal is to develop an algorithm for which this time is $O(N^p)$ with p < 1.

Our algorithm groups the functions in (27) into blocks. We denote the number of functions in a block by b. Let

$$F_j = f_{(j-1)b+1} \circ f_{(j-1)b+2} \circ \cdots \circ f_{jb}$$
 (28)

If we write k as k = mb + l with $0 \le l < b$, then we have

$$z_k = F_1 \circ F_2 \circ \cdots \circ F_m \circ f_{mb+1} \circ f_{mb+2} \circ \cdots \circ f_{mb+l}(0)$$
(29)

The number of compositions in (29) is smaller than the number in (27) by roughly a factor of b if b is smaller than m, i.e., if k is bigger than b^2 .

Unfortunately, even though the f_i are explicit and relatively simple, the F_j cannot be explicitly computed. Our strategy is to approximate the f_i by functions whose compositions can be explicitly computed to give an explicit approximation to F_j . For large z, $f_i(z)$ is given by its Laurent series about ∞ . One could approximate f_i by truncating this Laurent series. Our approximation is of this nature, but slightly different.

Let $\gamma:[0,t]\to\mathbb{H}$ be a simple curve in the upper half plane with $\gamma(0)=0$. Let f(z) be the conformal map from \mathbb{H} onto $\mathbb{H}\setminus\gamma[0,t]$. We assume that f is normalized is the same way as our f_i , i.e., $f(\infty)=\infty$, $f'(\infty)=1$ and $f(0)=\gamma(t)$. Let a,b>0 be such that [-a,b] is mapped onto the slit $\gamma[0,t]$. Then f is real valued on $(-\infty,-a]\cup[b,\infty)$, and so f has an analytic continuation to $\mathbb{C}\setminus[-a,b]$ by the Schwartz reflection principle. We denote this extension by just f.

Let $R = \max\{a, b\}$, so f is analytic on $\{z : |z| > R\}$ and maps ∞ to itself. Thus f(1/z) is analytic on $\{z : 0 < |z| < 1/R\}$. Since our assumptions on f imply it has a simple pole at the origin with residue 1, we have

$$f(1/z) = 1/z + \sum_{k=0}^{\infty} c_k z^k$$
 (30)

This gives the Laurent series of f about ∞ .

$$f(z) = z + \sum_{k=0}^{\infty} c_k z^{-k}$$
 (31)

This Laurent series is a natural approximation to use for f when z is large. However, we will use a different but closely related representation.

Define $\hat{f}(z) = 1/f(1/z)$. Since f(z) does not vanish on $\{|z| > R\}$, $\hat{f}(z)$ is analytic in $\{z : |z| < 1/R\}$. Our assumptions on f imply that $\hat{f}(0) = 0$ and $\hat{f}'(0) = 1$. So \hat{f} has a power series

$$\hat{f}(z) = z + \sum_{j=2}^{\infty} a_j z^j \tag{32}$$

The radius of convergence of this power series is easily shown to be 1/R. Note that the coefficients of the power series of \hat{f} are the coefficients of the Laurent series of 1/f.

The primary advantage of our power series over the Laurent series is its behavior with respect to composition.

$$(f_1 \circ f_2)\hat{}(z) = \frac{1}{f_1((f_2(1/z)))} = \frac{1}{f_1(1/\hat{f}_2(z))} = \hat{f}_1(\hat{f}_2(z))$$
(33)

Thus

$$(f_1 \circ f_2)^{\hat{}} = \hat{f}_1 \circ \hat{f}_2 \tag{34}$$

Our approximation for f(z) is to approximate $\hat{f}(z)$ by the truncation of its power series at order n. So

$$f(z) = \frac{1}{\hat{f}(1/z)} \approx \left[\sum_{j=0}^{n} a_j z^{-j}\right]^{-1}$$
 (35)

For each f_i we compute the power series of \hat{f}_i to order n. Using these and (34), we compute the power series of \hat{F}_j to order n. Let $1/R_j$ be the radius of convergence for the power series of \hat{F}_j . Now consider evaluating the composition in equation (29). Let z be the argument to F_j . If z is large compared to R_j , then $F_j(z)$ is well approximated using the power series of \hat{F}_j . We introduce a parameter L > 1 and use the power series of \hat{F}_j to compute $F_j(z)$ whenever $|z| \geq LR_j$. When $|z| < LR_j$, we just use (28) to compute $F_j(z)$. The argument of F_j is random, and so whether or not we can approximate a particular F_j using these power series is random. As part of the algorithm we must compute R_j . This is easy. R_j is the smallest positive number such that $F_j(R_j)$ and $F_j(-R_j)$ are both real.

In addition to the choice of simple curves we use (tilted slits, vertical slits,), there are three parameters in our algorithm. b is the number of functions composed in a block. n is the order at which we truncate our series approximation. L is the scale that determines when we use series for F_j . The parameter b has little effect on the accuracy of the algorithm and we

should choose it to make the algorithm run as quickly as possible. Eq. (29) suggests that b should vary with N as \sqrt{N} and experiments bear this out.

The choice of n involves a tradeoff of speed vs. accuracy. Larger n means more terms in the series, hence slower but more accurate computations. We typically use n = 12.

The parameter L will determine how fast the series converges. Roughly speaking, the series will converges at least as fast as the geometric series $\sum_n L^{-n}$. The choice of L also involves a tradeoff of speed vs. accuracy. Larger L means the series converges faster and so is more accurate. But it also means that we use the block functions F_j less frequently, and so the computation is slower. We typically use L=4.

A detailed study of the effects of the choices of b, n and L can be found in [12]. This paper also studies the time to compute a point on the curve and finds it is $O(N^p)$ with p approximately 0.4. To illustrate the accuracy of our series approximation we compute an SLE curve for $\kappa = 6$ with and without the series approximation. We use the same Brownian motion sample path for both curves. We typically take n = 12 and L = 4. With these choices the difference between the curves obtained with and without the series approximation is extremely small and cannot be seen in plots of the curves. If we reduce n to only 6 we can begin to see the effect of the series approximation. Figure 7 shows the two curves we get for $\kappa = 6$ and the same sample of the driving process when we use n = 6. One can only distinguish the difference in the enlargement and even then it is small.

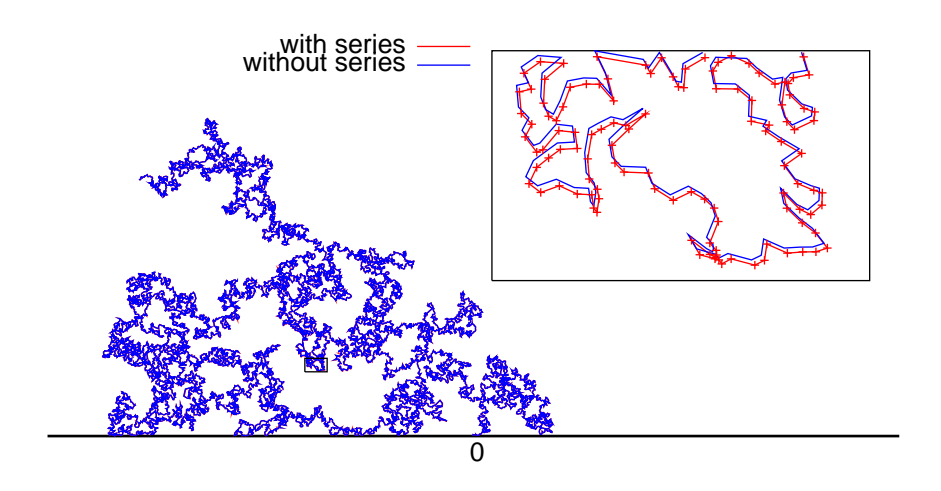


Figure 7: Two curves for SLE with $\kappa = 6$ are shown. They use the same Brownian motion sample path but one uses the series approximation and the other does not.

We now consider the algorithm for computing the driving function of a given curve. The number of operations needed to compute a single w_{k+1} is proportional to k. So to compute all the points w_{k+1} , and hence the approximation to the driving function, requires a time $O(N^2)$. The idea for improving this is the same as before - we group the functions we are composing into blocks and approximate the composition F of the functions in a block using the power series of \hat{F} . The only minor difference is that the order of the conformal maps in (22) is the opposite of that in (20). We continue to denote the number of functions in a block by b. Let

$$H_j = h_{jb} \circ h_{jb-1} \circ \dots \circ h_{(j-1)b+2} \circ h_{(j-1)b+1}$$
 (36)

If we write k as k = mb + r with $0 \le r < b$, then (22) becomes

$$w_{k+1} = h_{mb+r} \circ h_{mb+r-1} \circ \cdots \circ h_{mb+1} \circ H_m \circ H_{m-1} \circ \cdots \circ H_1(z_{k+1})$$

$$\tag{37}$$

As before, the h_i are relatively simple, but the composition H_j cannot be explicitly computed. We approximate h_i by the power series of $\hat{h_i}$ and compute the approximations to the compositions in (36) just once rather than every time we compute a w_k .

Recall that h_i is normalized so that $h_i(\infty) = \infty$ and $h'_i(\infty) = 1$. It maps \mathbb{H} minus a simple curve near the origin to \mathbb{H} , sending the tip of the curve to the origin. Let h denote such a conformal map. Let R be the largest distance from the origin to a point on the curve. Then h is analytic on $\{z \in \mathbb{H} : |z| > R\}$. Since h is real valued on the real axis, the Schwarz reflection principle says it may be analytically continued to $\{z \in \mathbb{C} : |z| > R\}$. Moreover, it does not vanish on this domain. We could approximate h by its Laurent series about ∞ , but as with the first algorithm it is better to use the power series of $\hat{h}(z) = 1/h(1/z)$. Note that the radius of convergence of this power series is 1/R.

As before, the advantage of working with the power series of \hat{h} is its behavior with respect to composition: $(h_1 \circ h_2)^{\hat{}} = \hat{h_1} \circ \hat{h_2}$ Our approximation for $h_i(z)$ is to replace $\hat{h_i}(z)$ by the truncation of its power series at order n as we did in eq. (35). The approximation of h_i and of H_j proceeds as for the first algorithm. For each h_i we compute the power series of $\hat{h_i}$ to order n. We then use them to compute the power series of $\hat{H_j}$ to order n. As before we introduce a parameter L > 0. Let $1/R_j$ be the radius of convergence for the power series of $\hat{H_j}$. Now consider equation (37). If the argument z of H_j satisfies $|z| \geq LR_j$, then we approximate $H_j(z)$ using the power series of $\hat{H_j}$. Otherwise we just use (36) to compute $H_j(z)$. The argument of H_j is random, so as before whether or not we can approximate a particular H_j by its series is random.

We need to compute R_j . Consider the images of $z_{(j-1)b}, z_{(j-1)b+1}, \cdots z_{jb-1}$ under the map $H_{j-1} \circ H_{j-2} \circ \cdots \circ H_1$. The domain of the conformal map H_j is the half-plane $\mathbb H$ minus some curve Γ_j which passes through the images of these points. The radius R_j is the maximal distance from the origin to a point on Γ_j . This distance should be very close to the maximum distance from the origin to images of $z_{(j-1)b}, z_{(j-1)b+1}, \cdots z_{jb-1}$ under $H_{j-1} \circ H_{j-2} \circ \cdots \circ H_1$. So in our algorithm we approximate R_j by the maximum of these distances.

To compute the driving function without using the power series we must compute all the points w_k . So if we do not use the power series, the time needed is $O(N^2)$. The improvement

in the speed of the algorithm from using the power series approximation is studied in [13]. Numerical experiments indicate it is $O(N^p)$ with p approximately equal to 1.35.

7 Conclusions and open problems

We have reviewed numerical methods for taking a driving function and finding the curve produced by the Loewner equation and for taking a curve in the half plane and finding the corresponding driving function. Both methods are based on approximating the driving function over short time intervals by a function for which the Loewner equation may be solved explicitly. The solution of the Loewner equation over the entire interval is then given by a composition of such maps. Our numerical studies used as the simple maps the conformal maps that produce a vertical slit or a tilted slit in the half plane. The difference in the results when we use vertical slits or tilted slits is small. The vertical slit map is considerably faster and simpler to implement, so we see no reason to use the tilted slit map. To simulate SLE effectively it is imperative that the choice of time intervals be done in a way that depends on the sample of the driving function so that sections of the curve that correspond to small changes in capacity are computed accurately.

The speed of both algorithm can be greatly increased by using power series approximations of certain analytic functions. This approximation is quite accurate and the errors from it are insignificant compared to the effect of changing the number of points used on the curve or compared to the difference between using vertical slits or tilted slits in the algorithm.

We end with a discussion of a variety of open problems related to these two algorithms.

We have only discussed the simulation of chordal SLE. In chordal SLE the random curve goes between two boundary points, e.g., the origin and infinity in the half plane. In radial SLE the random curve goes between a boundary point and an interior point, e.g., the point 1 and the origin in the unit disc. The simulation of radial SLE is similar. Can one use the ideas we used to speed up the simulation of chordal SLE to speed up the simulation of radial SLE?

Instead of taking the scaling limit at the critical point, one can consider off critical models and take the scaling limit in such a way that it has a finite correlation length. What can you say about the driving process for this scaling limit? For percolation it is know to be rather nasty [18]. See also [4, 8].

There are several methods for numerically computing the conformal map of a given simply connected domain onto a standard domain, like the unit disc. One of these methods, the zipper algorithm [14, 16], reduces the problem to that of finding the conformal map from the half plane minus a curve to the half plane. So the power series approximation that we use also provides a faster version of this algorithm. How does this faster version compare to other methods for finding the conformal map from a simply connected domain to a standard domain [10, 22]?

As discussed in section 2, it is natural to conjecture that the discrete SLE curve $\hat{\gamma}$ introduced in that section converges to the SLE curve for $\kappa \leq 4$ and converges to the SLE trace which generates the SLE hull for $\kappa > 4$. Prove this. Part of the problem is figure out the sense in

which they converge.

For the inverse problem of finding the driving function for a given curve, there is an analogous convergence question. Show that as the number of points used to approximate the curve goes to infinity, the computed driving function converges to the true driving function. Marshall and Rohde have proved convergence for a particular variant of the zipper algorithm [16].

As discussed in section 4, there is a certain stability to our approximation of the curve generated by a given driving function. Explain this stability.

Acknowledgments:

I thank Don Marshall and Stephen Rohde for useful discussions. Talks and interactions during visits to the Banff International Research Station in March and May of 2005 and to the Kavli Institute for Theoretical Physics in September, 2006 contributed to the research included in these notes. The opportunity to present this material at the 2008 Enrage summer school at IHP is warmly acknowledged. This research was supported in part by the National Science Foundation under grants DMS-0201566 and DMS-0501168.

References

- [1] C. Amoruso, A. K. Hartman, M. B. Hastings, and M. A. Moore, Conformal invariance and SLE in two-dimensional Ising spin glasses, *Phys. Rev. Lett.* **97**, 267202 (2006). Archived as arXiv:cond-mat/0601711.
- [2] R. Bauer, Discrete Loewner evolution, Annales de la Faculté des Sciences XII 433-451 (2003). Archived as arXiv:math.PR/0303119.
- [3] M. Bauer, D. Bernard, 2D growth processes: SLE and Loewner chains, *Phys. Rept.* 432, 115-221 (2006). Archived as arXiv:math-ph/0602049.
- [4] M. Bauer, D. Bernard, and K. Kytölä, LERW as an example of off-critical SLE's. Archived as arXiv:0712.1952.
- [5] D. Bernard, G. Boffetta, A. Celani, and G. Falkovich, Conformal invariance in two-dimensional turbulence, *Nature Physics* **2**, 124 (2006). Archived as arXiv:nlin.CD/0602017.
- [6] D. Bernard, G. Boffetta, A. Celani, and G. Falkovich, Inverse turbulent cascades and conformally invariant curves. Archived as arXiv:nlin.CD/0609069.

- [7] D. Bernard, P. Le Doussal, and A. A. Middleton, Are domain walls in 2D spin glasses described by stochastic Loewner evolutions?, *Phys. Rev. B* **76**, 020403(R) (2007). Archived as arXiv:cond-mat/0611433.
- [8] F. Camia, L. Fontes, and C. Newman, The scaling limit geometry of near-critical 2d percolation. Archived as arXiv:cond-mat/0510740.
- [9] J. Cardy, SLE for Theoretical Physicists, Ann. Phys. 318, 81-118 (2005). Archived as arXiv:cond-mat/0503313.
- [10] T. Driscoll and L. Trefethen, *Schwarz-Christoffel Mapping*, Cambridge University Press, 2002.
- [11] W. Kager, B. Nienhuis, A Guide to Stochastic Loewner Evolution and its Applications, J. Statist. Phys. 115, 1149-1229 (2004). Archived as arXiv:math-ph/0312056.
- [12] T. Kennedy, A fast algorithm for simulating the chordal Schramm-Loewner evolution, *J. Statist. Phys.* **128**, 1125–1137 (2007). Archived as arXiv:math.PR/0508002.
- [13] T. Kennedy, Computing the Loewner driving process of random curves in the half plane, J. Statist. Phys. 131, 803–819 (2008). Archived as arXiv:math/0702071
- [14] R. Kühnau, Numerische Realisierung konformer Abbildungen durch "Interpolation", Z. Angew. Math. Mech. 63, 631-637 (1983).
- [15] G. Lawler, Conformally Invariant Processes in the Plane, Mathematical Surveys and Monographs, vol. 114, American Mathematical Society, 2005.
- [16] D. E. Marshall and S. Rohde, Convergence of a variant of the Zipper algorithm for conformal mapping, SIAM J. Numer. Anal. 45, 2577–2609 (2007).
- [17] D. E. Marshall and S. Rohde, The Loewner differential equation and slit mappings, *Jour. Amer. Math. Soc.* **18**, 763-778 (2005).
- [18] P. Nolin, W. Werner, Asymmetry of near-critical percolation interfaces, *J. Amer. Math. Soc.* 22, 797–819 (2009). Archived as arXiv:0710.1470.
- [19] S. Rohde, private communication (2005).
- [20] S. Rohde, O. Schramm, Basic properties of SLE, Ann. of Math. 161, 883–924 (2005). Archived as arXiv:math.PR/0106036.
- [21] O. Schramm, Scaling limits of loop-erased random walks and uniform spanning trees, *Israel J. Math.* 118, 221–288 (2000). Archived as arXiv:math.PR/9904022.

- [22] J. Tsai, The Loewner driving function of trajectory arcs of quadratic differentials, *J. Math. Anal. Appl.*(to appear). Archived as arXiv:0704.1933v2.
- [23] W. Werner, Random planar curves and Schramm-Loewner evolutions Springer Lecture Notes **1840**, 107-195 (2004). Archived as math.PR/0303354 in arXiv.org.